Quantum Chemical Reaction Path and Transition State for a Model Cope (and Reverse Cope) Elimination

Istvan Komaromi[†] and Jean M. J. Tronchet*

Pharmaceutical Organic Chemistry, Sciences II, 30, Quai E.-Ansermet, CH-1211 Geneva 4, Switzerland

Received: February 19, 1997[⊗]

Ab initio and density functional calculations have been performed on a simple model of the Cope and reverse Cope elimination reactions. The correlational energies have been taken into account up to the MP4(SDQ)/6-311G** and CCSD(T)/6-311++G** levels for RHF methods or using different (nonlocal) exchange and correlation functionals for the density functional theory. The calculated activation energies and free energies for both hydrogenated and deuterated reagents were found to be in good agreement with the available experimental data as well as primary kinetic isotope effects. The bond order analysis predicts an almost completely synchronous reaction path for correlated methods and a little advanced H transfer for the HF method. The intrinsic reaction coordinate path following method shows that although the reaction is concerted, the H transfer slightly precedes the C−N bond breaking. Modeling the solvent effect explained the solvent dependence of the Cope (reverse Cope) products equilibrium. Any very significant hydrogen tunneling could be excluded from the shape of the Born−Oppenheimer potential energy surface and from the good agreement between the calculated and measured primary kinetic isotope effects. From these results and the computed minimal energy path, a refined picture of both the Cope and reverse Cope eliminations implying a one-step slightly dissymmetric reaction mechanism could be proposed.

Introduction

The amine oxide thermolysis leading to olefins, known as the Cope elimination[1] (Scheme 1), is widely used in preparative organic chemistry. The reverse (retro) reaction path is also known, but until recent years, only a few applications had been reported.[2−4] The reaction mechanism of the Cope elimination has been carefully studied by several authors mainly by means of primary kinetic isotope effect measurements.[5−7] From these results, a five-membered cyclic synchronous transition state (TS) with a *ca.* 120° C···H···O angle is generally accepted for this reaction (Scheme 1). Concerning the retro reaction, both a radical chain[2] and a concerted mechanism (the microscopic reverse of that of the Cope elimination) implying synchronous C−N and C−H bond formations[8−11] have been proposed. The synchronous mechanism is now most generally accepted[8−10] although explicit solvent (DMSO) participation in the reaction mechanism has been also proposed.[7] It is known from the literature[9] that upon changing the solvent, the equilibrium can be shifted into the direction of either the Cope elimination or the reverse Cope elimination. A more polar solvent is favorable for the retro reaction path, because the polar retro Cope product is more efficiently solvated. On the other hand, the primary kinetic isotope effect measured for the Cope elimination was also found to be sensitive to the solvent: there was a small temperature dependency observed in DMSO[7] while it was practically independent from the temperature in diglyme.[12]

Despite the increasing interest in the retro Cope reaction,[9,10,13−17] we could not find in the literature any quantum chemistry analysis of either the Cope reaction or its retro variant.

We have conducted such a study in order to:

(1) compare the quantum chemical transition state structure with its currently admitted description inferred from experimental results,

SCHEME 1

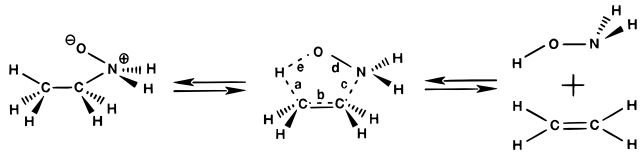

(2) analyze the "bent hydrogen transfer" theory implied in the classical mechanism of the Cope elimination and determine which nuclear movements take place along the retro path,

(3) monitor the structural variations taking place when following the minimal energy path on the Born−Oppenheimer surface,

(4) compare the quantum chemically derived values obtained at different levels of theory both to each other and to those inferred from experimental results, to propose a refined picture of both of these reaction mechanisms, and finally

(5) determine how the solvent, modeled either as a polarizable continuum or as being explicitly involved in the reaction, can influence the reaction mechanism.

Computational Details

General Strategy. The potential energy surface over the rectangular grid spanned by the forming C−H and C−N bonds in the 1.0−2.2 and 1.4−2.6 Å ranges respectively was calculated. From this, the molecular orientation on the Born−Oppenheimer surface before the transition state (retro point of view) was obtained and the approximate minimal energy reaction path was determined. It was also used to search for alternative reaction paths. The approximate transition state derived from the potential energy surface was then optimized using the eigenvector following algorithm implemented into the GAUSSIAN94[18] and 92[19] packages. In all cases where analytical methods were available (HF, MP2, and density functional levels), the transition states were checked for the presence of one and only one negative frequency while no negative

[†] Present address: Emory University, Chemistry Department, 1515 Pierce Drive, Atlanta, Georgia 30322.

[⊗] Abstract published in *Advance ACS Abstracts,* April 15, 1997.

S1089-5639(97)00617-8 CCC: $14.00

TABLE 1: Geometrical Parameters (*a*−*e* Bond Lengths in Å, *ae* Bond Angle between *a* and *e* Bonds in deg: Rotations Correspond to Scheme 1) of the Transition State of the Cope Elimination and Its Retro Variant

	parameter					
method	*a*	*b*	*c*	*d*	*e*	*ae*
HF/6-31G**	1.4580	1.4210	1.8244	1.3425	1.1541	145.8
MP2/6-31G**	1.3624	1.4051	1.9789	1.3456	1.2314	148.6
MP2/6-311++G**	1.3640	1.4118	1.9470	1.3374	1.2283	147.9
MP4/6-31G**	1.3592	1.4134	1.9868	1.3536	1.2408	148.9
MP4(SDQ)(fc)/6-311G**	1.3902	1.4186	1.9253	1.3446	1.2021	148.6
MP4(SDQ)(fc)/6-311G**	1.3902	1.4186	1.9253	1.3446	1.2021	148.6
QCISD/6-31G**	1.3618	1.4124	1.9952	1.3558	1.2294	149.6
B3LYP/6-31G**	1.3523	1.4096	2.0465	1.3422	1.2604	149.3
B3LYP/6-311++G**	1.3361	1.4096	2.0558	1.3420	1.2790	148.8
BLYP/6-31G**	1.3407	1.4162	2.1629	1.3559	1.2907	150.9
BP86/6-31G**	1.3680	1.4122	2.1140	1.3841	1.2506	150.6
CASSCF/6-31G**	1.4190	1.4066	1.9589	1.3849	1.2113	149.5

TABLE 2: SCF/6-31G Bond Orders of the Bonds Directly Involved in the Cope Elimination and Its Reverse Variant at the Transition State and for the Reactants (Products) of These Reactions Using the HF/6-31G** and MP2/6-31G** Geometries**

	HF geometry					MP2 geometry				
	C−H	C−N	O−H	C−C	N−O	C−H	C−N	O−H	C−C	N−O
hydroxylamine			0.866		0.898			0.861		0.900
ethylene				1.969					1.968	
transition state	0.431	0.455	0.441	1.264	0.997	0.462	0.402	0.389	1.296	1.004
retro product	0.952	0.835		0.969	0.972	0.948	0.828		0.968	0.983

frequencies were found for the stable energy minima. This was assumed in the other cases.

Quantum Mechanical Methods. The density functional calculations have been performed using Becke's gradient-corrected exchange functional[20,21] combined with either the Lee−Yang−Parr[22] or Perdew's[23] gradient-corrected correlation functionals (BLYP or BP86 methods in the Gaussian94 package). Becke's three-parametric hybride exchange functional[24] with the Lee−Yang−Parr correlation functional[22] has also been used (Becke3LYP method in Gaussian94 and B3LYP hereafter). For the MPn and QCISD calculations, the frozen core approximation was applied. In the case of CCSD(T)/6-311++G** (single-point) calculations, all the electrons were allowed to correlate. For the CASSCF calculations—only used to justify the adequacy of the single reference based methods and to calculate the transition state—the selected orbitals in the active space were the Lp (N) and σ (OH) on the hydroxylamine moiety, the π (CC) on the ethylene part, and two virtual orbitals on each moiety, this constituting a six-electrons-in-seven-orbitals CASSCF set. In order to estimate the open shell contribution to the wave function, calculations starting from totally different α and β orbitals, originated in the triplet wave functions, were also performed, but in every case, the corresponding RHF solution was obtained. Similarly, CASSCF calculations revealed a very dominant contribution from the reference (more than 95%).

The kinetic isotope effect has been calculated at 298, 348, and 398 K, using the thermodynamic formulation[25] on the basis of the Gibbs free energy values obtained from the frequency calculations for both the transition state and the reactants (or products, depending on the direction). The transmission factor was supposed to be the same for both isotopes, and no tunneling effect was calculated.

The solvent effect was calculated using a continuum solvation model. In order to calculate the influence of the solvent upon the kinetic isotope effect, the Onsager solvation model was applied.[26] For a more precise estimation of the solvent effect on the molecular geometries and energies, the self-consistent isodensity polarized continuum model (SCIPCM), developed by Wiberg *et al.*[27,28] on the basis of Tomasi's polarizable continuum model,[29] was applied.

To follow the minimal energy path (MEP), FUKUI's[30] intrinsic reaction coordinate (IRC) calculations, using the Gonzalez−Schlegel algorithm[31,32] implemented in the GAUSSIAN94 package,[18] have been performed starting from the transition state and proceeding along the reaction coordinate in both Cope and retro Cope directions. The step size was chosen as 0.15 amu$^{1/2}$ bohr. The bond order analysis proposed by Mayer[33,34] has been performed using the GAMESS(US) package.[35]

The standard 6-31G**,[36,37] 6-311G**,[38] and 6-311++G**[38,39] basis sets were used throughout this study.

Results and Discussion

The interatomic distances for the cyclic transition state structure (Scheme 1) have been calculated at different levels of theory (Table 1). The results indicate an important contribution from the dynamical electron correlation to the TS geometry, particularly for the breaking and forming bonds, *i.e.* the CASSCF method which calculates the nondynamical electron correlation and only partially (depending on the active space) the dynamical electron correlation affords values intermediate between those of HF on one hand and the MPn, QCISD, and DFT methods on the other hand. It can also be observed that increasing either the basis set or the electron correlation above MP2/6-31G** has a small effect only on the TS geometry. Methods taking into account electron correlation indicate approximatively symmetrical bond-breaking and bond-forming processes, whereas the HF method favors an advanced C−N bond formation relative to the hydrogen transfer. This is particularly apparent from Table 2 where the Mayer's bond orders[33,34] calculated for the TS and the stable end products are collected.

Examining the potential energy surface (Figure 1) indicates that the approximate synchronous reaction mechanism corresponds to the minimum energy path even if the potential energy surface is almost flat in the vicinity of the TS, which leaves open the possibility of some deviation from this scheme.

Figure 2 represents the O···H distances in the same coordinate systems as in Figure 1, this adding a fourth dimension to Figure 1. From these two graphs, it appears that no notable hydrogen-

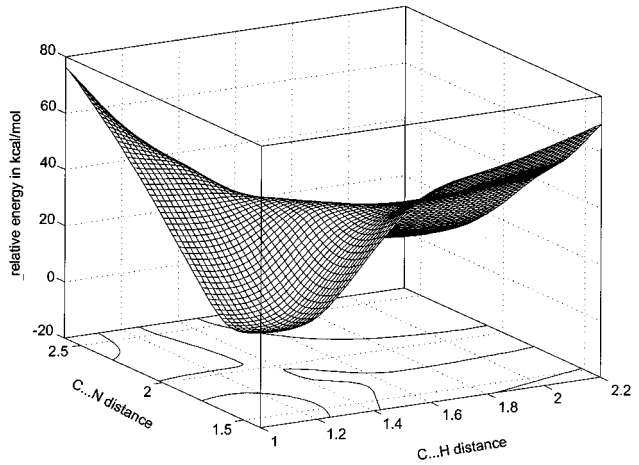

Figure 1. Potential energy surface (in kcal/mol) as a function of the length (in Å) of the two (C···H and C···N) breaking/forming bonds.

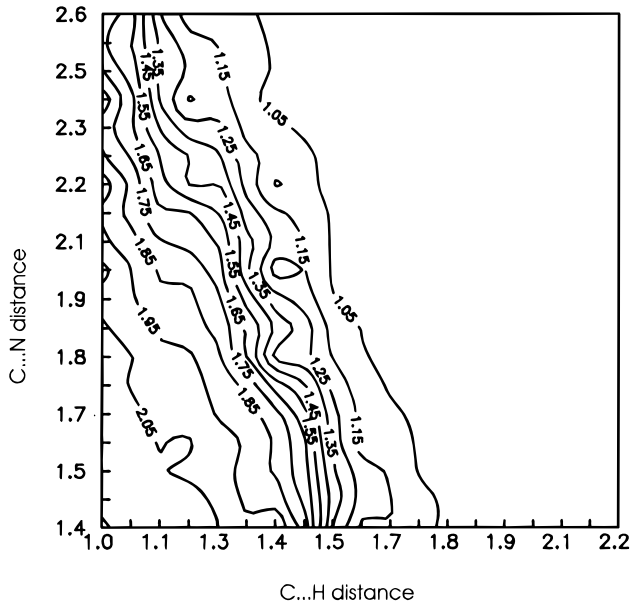

Figure 2. O···H bond length (in Å) as a function of the length of the two (C···H and C···N) breaking/forming bonds.

tunneling effect can be expected. Such a C−H → O−H tunneling with a constant C−N bond length in the usual 1.4−1.5 Å range would lead to a structure located on a high-energy area of the surface without any local minimum. It has a very small probability. That means also that the rate-determining step of the reaction is not a simple proton transfer. On the other hand, next to the saddle point, where the width of the potential energy surface is smaller and the tunnel would connect two lower energy points, the feasibility of such tunneling cannot be excluded.

All applied methods predicted that in the TS the five participating atoms (C═C and N−O−H) were located in the same plane. It is also worth mentioning that the conformation of the hydroxylamine needed to enter the retro reaction corresponds to that of the minimum energy. This is not only true for our simple model but also for the mono- and di-N-substituted derivatives as established by experimental[40−43] or theoretical[44−46] methods. In these conditions, the retro reaction does not need any extra activation energy to populate the reacting conformation.

The computed values of the activation energies (Table 3) appear to heavily depend on the applied model. The highest values are obtained by the HF method whereas "pure" DFT methods afford, as expected for a reaction involving a proton transfer,[47] the lowest figures. The MPn, QCISD, and CCSD(T) results fall into the experimental value range.[6] It should however be stressed that experimental $\Delta H^{\ddagger}$ and $\Delta S^{\ddagger}$ figures are extremely sensitive to the nature of the solvent. For the Cope elimination both decrease with a reduction of the percentage of polar protic solvent in a polar protic/polar aprotic solvent mixture and the values corresponding to pure dimethyl sulfoxide ($\Delta H^{\ddagger} = 24.3$ kcal/mol, $\Delta S^{\ddagger} = -0.12$ eu) represent the upper limit for a reaction calculated in the vacuum. The ZPVE corrections tend to decrease the difference between the activation energies of the reactions proceeding in two opposite directions. Kinetic data computed at three different temperatures are collected in Table 4. In accordance with the low experimental absolute value of $\Delta S^{\ddagger}$ in an aprotic solvent,[6] the computed free energy of activation of the Cope elimination is almost insensitive to temperature variations. The $\Delta G^{\ddagger}$ values for the reverse Cope elimination are notably superior to those of the Cope elimination. As all reverse Cope reactions described to date are intramolecular reactions, the free energy term corresponding to a change in the number of chemical species should disappear, leveling the values of $\Delta G^{\ddagger}$ in either direction. The computation (Table 4) reproduces satisfactorily the kinetic isotope effect and the temperature dependence measured in DMSO.[7] The computed k_H/k_D values are intermediate between those measured in DMSO where they were interpreted as corresponding to a linear H transfer through the participation of one molecule of solvent[7] and those observed in diglyme.[12] In diglyme, however, a null temperature dependence of k_H/k_D was observed which led Kwart *et al.*[12] to favor a bent hydrogen transfer mechanism.

The imaginary vibration corresponding to the saddle point (Figure 3) corresponds either mostly to a O−H stretching with a small bending component or to a C−H stretching with a larger bending contribution. Coupled motions from the other nuclei correspond to the C−N and C−H bond formations involved in the reverse Cope elimination.

On the other hand, the solvent effects detailed above can be modeled by a continuum solvation model implemented in the Gaussian94 package. The results are given in Tables 5 and 6. In Table 5, the solvent effects on the activation energies, the relative free energies, and the primary kinetic isotope effects were given at three temperatures. It is immediately apparent that the more polar the solvent, the smaller the free energy difference between the Cope and reverse Cope products. It can also be observed that increasing the temperature usually increases the free energy differences between the Cope and retro Cope products, increases the retro Cope activation energy, and decreases the kinetic isotope effect.

The temperature dependence of the kinetic effect in DMSO can be predicted without any explicit participation of the solvent. We have performed quantum chemical analysis (not detailed here) on the structure proposed in ref 7 explicitly involving one DMSO molecule in the transition state (Scheme 2). It appears from these calculations that this structure does not exist, the S−O(N) bond breaking spontaneously.[48] Therefore, this seven-membered (with linear O···H···C bond) transition state is very improbable. However, the contradiction between the null kinetic isotope effect measured in diglyme and the non-negligible one (almost as large as that calculated for DMSO) predicted by the theory at $\epsilon = 5$ or $\epsilon = 10$ clearly shows that this solvation model for the Cope elimination is oversimplified. Moreover, since at the transition state the H transfer plays an important role, the assumption of an isotope independent transmission factor (and no tunneling effect) does not seem to be perfectly correct.

In Table 6, quite important effects on the transition state

TABLE 3: Electronic Energies (in Hartrees), ZVPE (in kcal/mol) of the Reactants and Products of the Cope Elimination and Reverse Cope Elimination and the Corresponding Activation Energies (in kcal/mol). The CCSD(T)(full)/6-311++G Energies Were Calculated at the MP4(SDQ)(fc)/6-311G** Geometries**

	compound											
	ethylene		hydroxylamine		retro product		transition state		activation energy		activation energy	
	energy	ZPVE	energy	ZPVE	energy	ZPVE	energy	ZPVE	(Cope)	ΔZPVE[a]	(r-Cope)	ΔZPVE[a]
HF/6-31G**	−78.038 841 5	34.194	−130.991 662 4	27.665	−209.027 468 2	66.462	−208.958 528 7	62.337	43.260	4.124	45.154	0.479
MP2/6-31G**	−78.317 281 9	32.847	−131.354 209 4	25.833	−209.677 827 7	63.602	−209.636 382 6	59.416	26.007	4.186	22.031	0.736
MP2/6-311++G**	−78.383 952 7		−131.467 303 5		−209.858 635 6		−209.816 655 5		26.343		21.712	
MP4/6-31G**	−78.344 639 6		−131.372 118 2		−209.718 877 7		−209.669 887 6		30.742		29.411	
QCISD/6-31G**	−78.346 169		−131.372 991 2		−209.720 835 7		−209.672 099 8		30.582		29.531	
B3LYP/6-31G	−78.593 797 9	32.072	−131.715 775 4	25.225	−210.314 175 9	61.424	−210.279 865 1	57.644	21.530	3.780	18.642	0.347
BLYP/6-31G**	−78.543 388 1	31.191	−131.682 151 6	24.121	−210.227 622 6	59.070	−210.202 584 7	55.398	15.716	3.672	14.404	0.087
BP86/6-31G**	−78.585 292	31.161	−131.719 747 4	24.327	−210.314 856 2	59.177	−210.290 336 3	55.761	15.386	3.416	9.226	0.273
B3LYP/6-311++G**	−78.615 537 7	31.861	−131.766 891 9	25.29	−210.384 563 4	61.332	−210.345 883 4	57.219	24.272	4.040	22.933	0.139
MP4(SDQ)(fc)/6-311G**	−78.371 631 6		−131.434 384 6		−209.807 115 9		−209.760 800 8		29.063		28.377	
CCSD(T)(full)/6-311++G**	−78.425 210 3		−131.495 973 2		−209.925 475 9		−209.879 655 2		28.753		26.059	

[a] ΔZPVE = ZPVE(transition state) − ∑(ZPVE(reactants)).

TABLE 4: Activation Energies ($\Delta E^{\ddagger}$), Enthalpies ($\Delta H^{\ddagger}$), and Free Energies ($\Delta G^{\ddagger}$) for the Cope and Reverse Cope Elimination, Activation Energy and Free Energy Shifts Induced by Replacement by Deuterium of the Transferred Hydrogen (Respectively $\Delta\Delta E^{\ddagger}$ and $\Delta\Delta G^{\ddagger}$) (kcal/mol) and k_H/k_D Ratios Calculated by the MP2/6-31G Method[a]**

T	reaction	$\Delta E^{\ddagger}$[b]	$\Delta H^{\ddagger}$	$\Delta G^{\ddagger}$	$\Delta\Delta E^{\ddagger}$	$\Delta\Delta G^{\ddagger}$	k_H/k_D
298	Cope elim.	22.272	22.101	22.492	0.655	0.720	3.373
	reverse Cope elim.	22.688	21.103	33.010	0.689	0.816	3.967
348	Cope elim.	22.272	22.121	22.555	0.655	0.732	2.882
	reverse Cope elim.	22.688	21.027	35.012	0.689	0.838	3.359
398	Cope elim.	22.272	22.150	22.616	0.655	0.742	2.555
	reverse Cope elim.	22.688	20.990	37.023	0.689	0.857	2.955

[a] Experimental values (in DMSO/ROH) for the Cope elimination: $\Delta H^{\ddagger}$ ∼24−30 kcal/mol, $\Delta\Delta E^{\ddagger}$ 0.695 kcal/mol. [b] The zero-point energy contribution is taken into account.

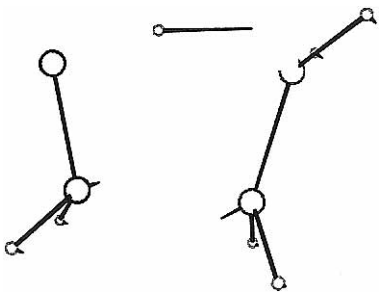

Figure 3. Imaginary vibration at the transition state calculated by the MP2/6-31G** method.

geometry caused by the SCIPCM solvation can be seen. It should be recognized that the transition state corresponds to an even more asynchronous reaction than that observed from the gas phase SCF calculations. The energy difference between the Cope and reverse Cope products is decreased by the solvent polarity, and the same effect was calculated for the activation free energy. Since no analytical second-derivative capability is available in the Gaussian94 program for the SCIPCM model, the corresponding free energy corrections were taken from the Onsager model.

Some water being usually present in DMSO, the explicit participation of one water molecule (or any R−OH group in other cases, where the solvent contains some alcohol) can also be considered (such a transition state was proposed by a referee) (Figure 4). The key interatomic distances are indicated for the RHF, B3LYP, and MP2 methods using the same 6-31G** basis. It is important to recognize that there is a rather large difference between the uncorrelated RHF method and the correlated ones while the latter show almost the same geometrical parameters even if the underlying theory treating the electron correlation is quite different. This means, on the other hand, that both methods predict probably more or less correct values. The HF method shows a rather product-like transition state from the H transfer point of view and a reactant-like transition state regarding the C−N and C═C bonds. The DFT and MP2 methods show a transition state in which the C−N bond breaking and the C═C double-bond forming are more advanced. In other words, the HF method describes the transition state as resembling an intermediate, while the other (B3LYP and MP2) methods predict structures which are more similar to a "real" transition state (although keeping some of the HF predicted "intermediate" character).

The energetics of this O−H group helped reaction can be found in Table 7. It can be seen that every applied method predicts this reaction to be unfavorable, compared to the five-membered mechanism implying no solvent participation. Every applied method (even the B3LYP one) predicts larger $\Delta G^{\ddagger}$ values than the experimental ones and (which is more important) larger than those found for the unimolecular reaction. On the other hand, the reverse Cope elimination was found especially unfavorable (although the total energy for the products and the reactants are almost the same) due to the large entropy effect in the $\Delta G^{\ddagger}$ value. These free energy differences were calculated for the trimolecular reaction which is extremely improbable. The more realistic bimolecular reaction, in which the hydroxylamine binds one water molecule in our model case, however, leads to even larger activation free energies, because this association decreases the free energy of the starting system.

Although in every case the transition states were proven by vibrational analyses and by checking the corresponding vibrational normal mode, which really pointed to a bond-breaking and bond-forming direction, the only proof that the transition state really binds the starting and forming compounds (on the potential energy surface) is the IRC analysis. This minimal

TABLE 5: Effect of Solvent Dielectric Constant (Using the Onsager Continuum Solvation Model) at the RHF//6-31G Level of Theory and of Reaction Temperature on the Calculated Activation Energies (*E**), the Free Enthalpy Differences Relative to the Cope (C) Product (ΔG), and the Primary Kinetic Isotope Effect. The Energies and Free Enthalpies Are Given in kcal/mol**

dielectric constant (ϵ)	temp/K	E^*(C)	E^*(rC)	ΔG(C)	$\Delta G^{\ddagger}_{rC}$	(k_H/k_D)C	(k_H/k_D)rC
1	298	43.260	45.170	16.054	55.828	3.362	4.620
	348	43.260	45.170	17.972	57.814	2.879	3.825
	398	43.260	45.170	19.895	59.803	2.562	3.317
5	298	44.419	42.920	12.787	53.708	3.132	4.304
	348	44.419	42.920	14.710	55.700	2.707	3.602
	398	44.419	42.920	16.647	57.705	2.423	3.138
10	298	44.629	42.451	12.142	53.286	3.054	4.196
	348	44.629	42.451	14.052	55.272	2.646	3.522
	398	44.629	42.451	15.989	57.267	2.376	3.079
20	298	44.744	42.192	11.781	53.059	3.002	4.134
	348	44.744	42.192	13.700	55.035	2.606	3.471
	398	44.744	42.192	15.637	57.040	2.344	3.038
40	298	44.802	42.049	11.580	52.925	2.974	4.095
	348	44.802	42.049	13.499	54.901	2.587	3.440
	398	44.802	42.049	15.452	56.921	2.325	3.016
60	298	44.830	42.010	11.503	52.877	2.958	4.073
	348	44.830	42.010	13.422	54.863	2.578	3.433
	398	44.830	42.010	15.375	56.874	2.318	3.007
80	298	44.830	41.982	11.474	52.858	2.958	4.069
	348	44.830	41.982	13.393	54.834	2.573	3.424
	398	44.830	41.982	15.347	56.845	2.312	3.002

TABLE 6: Influence of the Solvent Dielectric Constant Using the SCIPC Solvation Model at the RHF/6-31G Level of Theory on Energy (*E*, in hartrees) on Selected Interatomic Distances (in Å) of the Transition State and on the Relative Gibbs Free Energies[a] (in kcal/mol Relative to the Cope Product) of the Retro-Cope Product (ΔG_{rC}) and the Activation Free Energy[a] of the Retro Cope Reaction ($\Delta G^{\ddagger}_{rC}$)**

dielectric constant (ϵ)	E	r(O−H)	r(C−C)	r(C−N)	r(N−O)	r(C−H)	ΔG_{rC}	$\Delta G^{\ddagger}_{rC}$
1	−208.958 528 7	1.1541	1.4210	1.8244	1.3425	1.4580	16.05	55.83
10	−208.971 029 8	1.0903	1.4266	1.7880	1.3517	1.5560	9.06	53.33
20	−208.972 231 7	1.0834	1.4270	1.7852	1.3527	1.5688	8.37	53.04
40	−208.972 869 4	1.0798	1.4271	1.7853	1.3531	1.5757	8.01	52.90
60	−208.973 087 4	1.0787	1.4270	1.7842	1.3533	1.5781	7.91	52.86
80	−208.973 197 5	1.0781	1.4270	1.7841	1.3534	1.5793	7.83	52.86

[a] The statistical mechanical partitions were taken from the calculations carried out for the Onsager model.

SCHEME 2

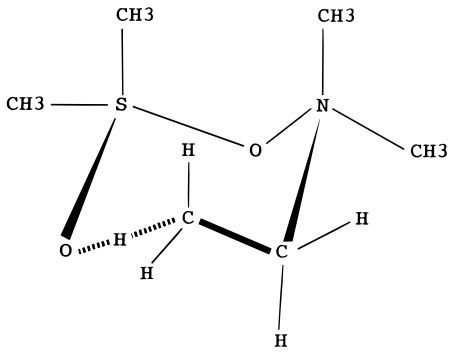

energy path, because of its minimal (=zero kinetic) energy nature, which is never satisfied in real reactions, does not exclude the existence of different reaction channels, but rather provides arguments in favor of one of them. Analyzing these trajectories and depicting some interatomic distances versus the reaction coordinate lead to some interesting conclusions regarding both models (unimolecular and −O−H group helped) of the studied reactions.

For the unimolecular, truly intramolecular, hydrogen transfer, the gas phase reaction path following calculation in mass-weighted coordinates clearly indicates (Figure 5) that the C−H and C−N bond formations as well as the O−H bond breaking are more or less simultaneous. However, in the vicinity of the TS, the C−H bond formation and the O−H bond breaking are the fastest processes in accordance with the computed vibrational

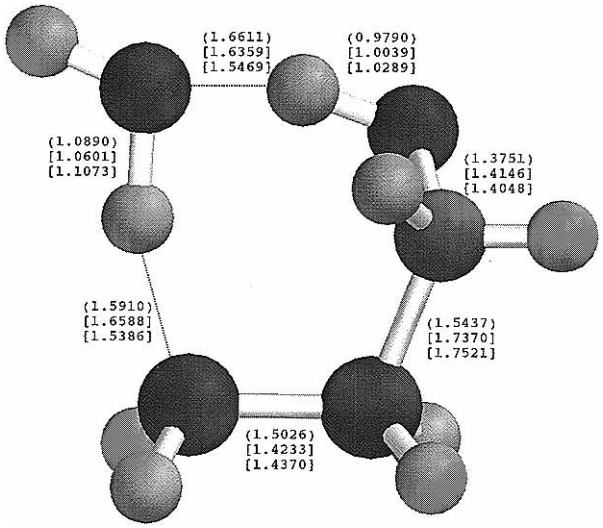

Figure 4. Alternate transition state with an explicit helper O−H group (modeled with one water molecule and calculated at RHF/6-31G**, B3LYP/6-31G**, and MP2/6-31G** levels of theory) for the Cope elimination.

motions. Contrarily, the C−N bond formation proceeds smoothly along the reaction coordinate. This indicates that on the minimal energy path, the different processes, even if monotonous, are not strictly synchronous at every point of the reaction coordinate. On the other hand, the C···H···O angle is almost invariant (*ca.* 150°) until the TS (Figure 6), decreasing rapidly from that point to its final value of *ca.* 125°. This represents, to a certain extent,

TABLE 7: Calculated Energies (in hartrees), Zero-Point Vibrational Energies (ZPVE), Electronic Part of the Activation Energies ($\Delta E^{\ddagger}$), Zero-Point Vibrational Energy Differences[a] (ΔZPVE), and Activation Free Energies ($\Delta G^{\ddagger}$) (all in kcal/mol) for the Cope and Reverse Cope Elimination[b] Using Different Methods

	H-bond complex		T		products		Cope elim			reverse Cope elim.		
method	energy	ZPVE	energy	ZPVE	energy	ZPVE	$\Delta E^{\ddagger}$	ΔZPVE	$\Delta G^{\ddagger}$	$\Delta E^{\ddagger}$	ΔZPVE	$\Delta G^{\ddagger}$
HF/6-31G**	−285.074 081 8	83.876	−284.984 547 0	80.577	−285.054 118 8	76.413	56.184	−3.299	53.834	43.657	4.164	67.256
B3LYP/6-31G**	−286.764 832 4	77.904	−286.697 545 5	74.006	−286.729 318 5	70.713	42.223	−3.898	38.805	19.938	3.292	42.620
MP2/6-31G**	−285.929 166	80.293	−285.851 963 7	76.687	−285.891 277 1	72.409	48.445	−3.606	45.237	24.668	4.278	48.367

[a] ΔZPVE = ZPVE(transition state) − Σ(ZPVE(reactants)). [b] Cope elimination started from the H-bonded complex, while the retro Cope elimination started from the Cope elimination products (hydroxylamine, water, and ethylene in our model reaction). More details can be found in the text.

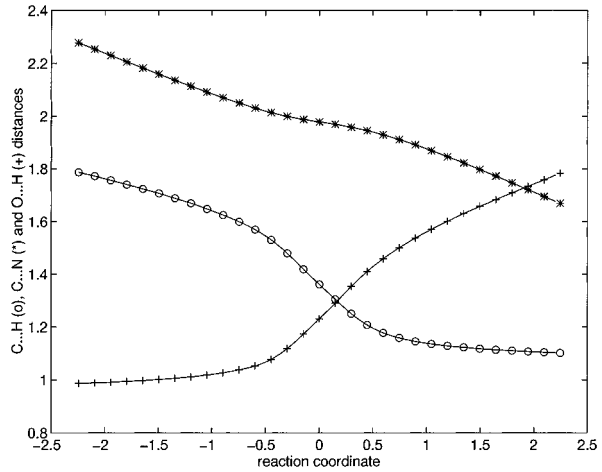

Figure 5. C···H (○), C···N (*), and O···H (+) distances (in Å) as a function of the mass-weighted intrinsic reaction coordinate (measured in (amu)$^{1/2}$ bohr).

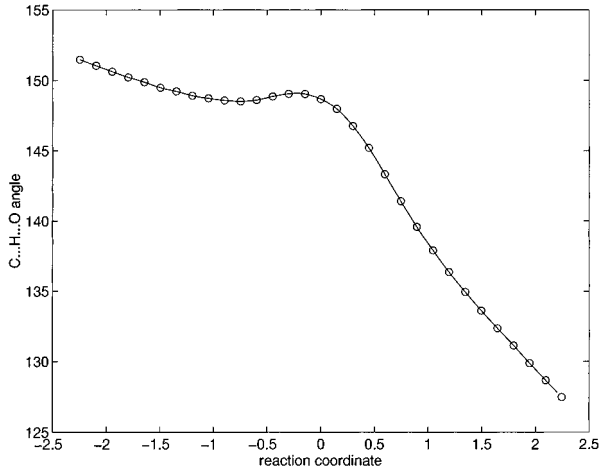

Figure 6. C···H···O angle (in deg) as a function of the mass-weighted intrinsic reaction coordinate (measured in (amu)$^{1/2}$ bohr).

the "bent hydrogen transfer" model of the Cope elimination. It should, however, be mentioned that other nuclear motions are coupled to this bending mode. The driving force for this reaction is, according to our opinion, an intramolecular attack—helped by an internal motion (vibration)—by the negatively charged aminoxide oxygen on the sterically available and still a little more tightly bound (due to the close electronegative group) hydrogen.

It is even more interesting to follow the minimal energy nuclear motions on the potential energy surface for the O−H group helped reaction starting from the left-hand side (hydrogen-bonded complex) of Figure 7. It can be clearly seen that first there is a proton shift from the bounded water to the aminoxid oxygen followed by another proton transfer from one of the C−H bonds to the O−H anion. When all these proton transfers are almost completed, the C−N bond will break. This is a very interesting mechanism in which the negative charge (like a ring

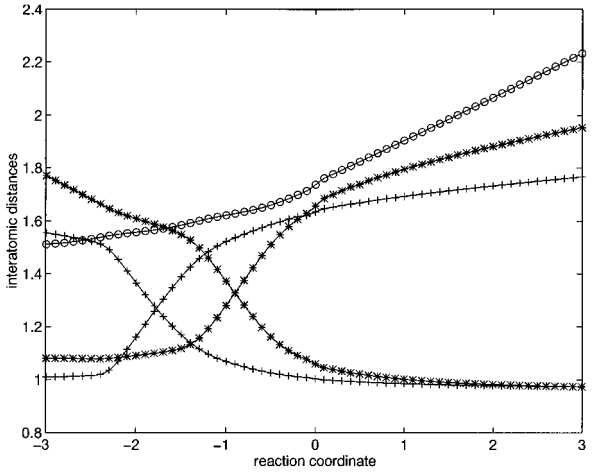

Figure 7. [HO−]H···O[−N] (+, starting from ∼1.6 Å), [H]O···H-[O−N] (+, starting from ∼1.0 Å), [C]C···H[OH] (*, starting from ∼1.8 Å), [C]C···H[OH] (*, starting from ∼1.1 Å), and [C]C···N (○) interatomic distances (in Å) as a function of the mass-weighted intrinsic reaction coordinate (measured in (amu)$^{1/2}$ bohr).

current) goes around the circle starting from the N−O oxygen and finishing on the N−O nitrogen. It is especially true from the results of the Hartree−Fock calculations, but the main features are similar from correlated calculations too. It should be mentioned that no intermediate (local minima) was found along the reaction path. In this case, the driving force for this reaction is the initial proton transfer step which is followed by a E1cB like elimination, almost typical from HF calculation or more or less so as shown by the correlated methods, in a way suggested by one of the referees. It seems, however, that this strongly asynchronous but one-step mechanism has no real advantages over the more synchronous hydrogen transfer.

Conclusion

The results of this computational study are in fair agreement with the experimental data in DMSO, without implying the DMSO molecule in the mechanism. The computed k_H/k_D values exhibit some similarity with those measured in diglyme. The computed transition states with its C···H···O angle of approximatively 140−150° predicted by all the applied methods is intermediate between those expected for "bent" and "linear" hydrogen transfer mechanisms. The HF method shows a hydrogen transfer slightly more advanced than the C−N bond breaking, while the effect of electron correlation on the transition structure leads to an approximately symmetrical (synchronous) mechanism. However, following the reaction path by Fukui's intrinsic reaction coordinate method shows that at the transition state the hydrogen transfer is slightly ahead of the C···N bond breaking. This picture is also in agreement with the vibrational normal mode of the imaginary frequency.

The solvent effect on the transition state (calculated using the continuum solvent model) can be characterized by a more advanced hydrogen transfer (from the Cope elimination point

of view) compared to the gas phase results (at least at the HF level of theory). Explicitly considering the solvent (DMSO or R−O−H molecules) shows that the transition state with participation of the DMSO molecule is very improbable while the O−H group mediated hydrogen transfer cannot be excluded but seems to be considerably less probable than the intramolecular one.

Although the substitution could slightly modify the situation, the mechanism of the Cope and reverse Cope eliminations can be characterized as one-step approximately synchronous reactions. The flatness of the potential energy surface in the vicinity of the transition state could explain the observed small solvent-induced mechanistic changes.

Acknowledgment. The authors thank Dr. M. W. Smith for a copy of the GAMESS(US) package. This work was generously supported by the Swiss Federal Office for Public Health and the Swiss National Research Foundation (Grants 3139-037156 and 20-43552.95).

References and Notes

(1) Cope, C.; Trumbull, E. R. *Org. React.* **1960**, *11*, 317.
(2) House, H. O.; Manning, D. T.; Melillo, D. G.; Lee, L. F.; Haynes, O. R.; Wilkes, B. E. *J. Org. Chem.* **1976**, *41*, 855.
(3) House, H. O.; Lee, L. F. *J. Org. Chem.* **1976**, *41*, 863.
(4) Oppolzer, W.; Siles, S.; Snowden, R.; Bakker, B. H.; Petrzilka, M. *Tetrahedron Lett.* **1979**, 4391.
(5) Bach, R. D.; Andrzejewski, D.; Dusold, L. R. *J. Org. Chem.* **1973**, *38*, 1742.
(6) Chiao, W.-B.; Saunders, W. H., Jr. *J. Am. Chem. Soc.* **1978**, *100*, 2802.
(7) Kwart, H.; Brechbiel, M. *J. Am. Chem. Soc.* **1981**, *103*, 4650.
(8) Ciganek, E. *J. Org. Chem.* **1990**, *55*, 3007.
(9) Ciganek, E.; Read, J. M., Jr.; Calabrese, J. C. *J. Org. Chem.* **1995**, *60*, 5795.
(10) Ciganek, E. *J. Org. Chem.* **1995**, *60*, 5803.
(11) Black, D. St. C.; Doyle, J. E. *Aust. J. Chem.* **1978**, *31*, 2317.
(12) Kwart, H.; George, T. J.; Louw, R.; Ultee, W. *J. Am. Chem. Soc.* **1978**, *100*, 3927.
(13) Oppolzer, W. *Pure Appl. Chem.* **1994**, *66*, 2127.
(14) Gravestock, M. B.; Knight, D. W.; Thornton, S. R. *J. Chem. Soc., Chem. Commun.* **1993**, 169.
(15) Fox, M. E.; Holmes, A. B.; Forbes, I. T., Thompson, M. *J. Chem. Soc., Perkin Trans 1*, **1994**, 3379.
(16) Woolhouse, A. D.; Gainsford, G. J.; Crump, D. R. *J. Heterocycl. Chem.* **1993**, *30*, 873.
(17) Tronchet, J. M. J.; Zsély, M.; Yazij, R. M.; Barbalat-Rey, F.; Geoffroy, M. *Carbohydr. Lett.* **1995**, *1*, 343.
(18) Frisch, M. J.; Trucks, G. W.; Schlegel, H. B.; Gill, P. M. W.; Johnson, B. G.; Robb, M. A.; Cheeseman, J. R.; Keith, T.; Petersson, G. A.; Montgomery, J. A.; Raghavachari, K.; Al-Laham, M. A.; Zakrzewski, V. G.; Ortiz, J. V.; Foresman, J. B.; Peng, C. Y.; Ayala, P. Y.; Chen, W.; Wong, M. W.; Andres, J. L.; Replogle, E. S.; Gomperts, R.; Martin, R. L.; Fox, D. J.; Binkley, J. S.; Defrees, D. J.; Baker, J.; Stewart, J. P.; Head-Gordon, M.; Gonzalez, C.; Pople, J. A. *Gaussian94, Revision B.3*; Gaussian Inc.: Pittsburgh PA, 1995.
(19) Frisch, M. J.; Trucks, G. W.; Schlegel, H. B.; Gill, P. M. W.; Johnson, B. G.; Wong, M. W; Foresman, J. B.; Robb, M. A.; Head-Gordon, M.; Replogle, E. S.; Gomperts, R.; Andres, J. L.; Raghavachari, K.; Binkley, J. S.; Gonzalez, C.; Martin, R. L.; Fox, D. J.; Defrees, D. J.; Baker, J.; Stewart, J. P.; Pople, J. A. *Gaussian92, Revision G.2*; Gaussian Inc.: Pittsburgh PA, 1995.
(20) Becke, A. D. *Phys. Rev. A* **1988**, *38*, 3098.
(21) Miehlich, B.; Savin, A.; Stoll, H.; Prauss, H. *Chem. Phys. Lett.* **1989**, *157*, 200 (transformed LYP funct.).
(22) Lee, C.; Yang, W.; Barr, R. G. *Phys. Rev. B* **1988**, *37*, 785.
(23) Perdew, P. *Phys. Rev.* **1986**, *33*, 8822.
(24) Becke, A. D. *J. Chem. Phys.* **1993**, *98*, 5648.
(25) Hirst, D. M. *A Computational Approach to Chemistry*; Blackwell Scientifics Publications Ltd: Oxford, London, 1990; p 243.
(26) Wong, M. W.; Wiberg, K. B.; Frisch, M. J. *J. Am. Chem. Soc.* **1991**, *113*, 4776.
(27) Wiberg, K. B.; Keith, T. A.; Frisch, M. J.; Murcko, M. *J. Phys. Chem.* **1995**, *99*, 9072.
(28) Foresman, J. B.; Keith, T. A.; Wiberg, K. B.; Snoonian, J.; Frisch, M. J. *J. Phys. Chem.* **1996**, *100*, 16098
(29) Miertus, S.; Scrocco, E.; Tomasi, J. *J. Chem. Phys.* **1981**, *55*, 117. Tomasi, J.; Bonaccorsi, R.; Cammi, R.; Valle F. O. *J. Mol. Struct.* **1991**, *234*, 401. Tomasi, J.; Persico, M. *Chem. Rev.* **1994**, *94*, 2027.
(30) Fukui, K. *Acc. Chem. Res.* **1981**, *14*, 363.
(31) Gonzalez, C.; Schlegel, B. *J. Chem. Phys.* **1989**, *90*, 2154.
(32) Gonzalez, C.; Schlegel, B. *J. Phys. Chem.* **1990**, *94*, 5523.
(33) Mayer, I. *Chem. Phys. Lett.* **1983**, *97*, 270.
(34) Mayer, I. *Theor. Chim. Acta* **1985**, *67*, 315.
(35) Schmidt, M. W.; Baldridge, K. K.; Boatz, J. A.; Elbert, S. T.; Gordon, M. S.; Jensen, J. H.; Koseki, S.; Matsunaga, N.; Nguyen, K. A.; Su, S. J.; Windus, T. L.; Dupuis, M.; Montgomery, J. A. *J. Comput. Chem.* **1993**, *14*, 1347.
(36) Hehre, W. J.; Ditchfield, R.; Pople, J. A. *J. Chem. Phys.* **1972**, *56*, 2257.
(37) Hariharan, P. C.; Pople, J. A. *Theor. Chim. Acta* **1973**, *28*, 213.
(38) Krishnan, R.; Binkley, J. S.; Seeger, R.; Pople, J. A. *J. Chem. Phys.* **1980**, *72*, 650.
(39) Clark, T.; Chandrrasekhar, J.; Spitznagel, G. W.; Schleyer, P. V. R. *J. Comput. Chem.* **1983**, *4*, 294.
(40) Rankin, D. W. H.; Todd, M. R.; Riddel, F. G.; Turner, E. S. *J. Mol. Struct.* **1981**, *71*, 171.
(41) Riddel, F. G.; Turner, E. S.; Rankin, D. W. H.; Todd, M. R. *J. Chem. Soc., Chem. Commun.* **1979**, 72.
(42) Fong, M. Y.; Johnson, L. J.; Harmony, M. D. *J. Mol. Spectrosc.* **1974**, *53*, 45.
(43) Sung, E.-M.; Harmony, J. *J. Mol. Spectrosc.* **1979**, *74*, 228.
(44) Tronchet, J. M. J.; Komaromi, I. *Int. J. Biol. Macromol.* **1993**, *15*, 69.
(45) Gange, D. M.; Kallel, E. A. *J. Chem. Soc., Chem. Commun.* **1992**, 824.
(46) Tronchet, J. M. J.; Komaromi, I. *J. Comput. Chem.* 1994, *15*, 1091.
(47) Barone, V.; Orlandini, L.; Adamo, C. *Chem. Phys. Lett.* **1995**, *15*, 295.
(48) Komaromi, I.; Tronchet, J. M. J. Unpublished results.